Title

In-situ/operando soft x-ray spectroscopy characterization of energy and catalytic materials

Permalink

https://escholarship.org/uc/item/97463217

Authors

Liu, Yi-Sheng
Feng, Xuefei
Glans, Per-Anders
et al.

Publication Date

2020-05-01

DOI

10.1016/j.solmat.2020.110432

In-situ/operando soft x-ray spectroscopy characterization of energy and catalytic materials

Yi-Sheng Liu, Xuefei Feng, Per-Anders Glans Suzuki, and Jinghua Guo
Advanced Light Source, Lawrence Berkeley National Laboratory, 1 Cyclotron Road

Abstract

The capabilities of soft x-ray absorption (XAS), soft x-ray emission spectroscopy (XES), resonant inelastic soft x-ray scattering (RIXS), and their application to characterization of solar energy materials are presented. We have discussed some recent developments of in-situ soft x-ray spectroscopy cells, which enable the investigation of critical solid/liquid or solid/gas interfaces in chemical and electrochemical processes under real-world practical conditions. In particular, in-situ soft x-ray spectroscopies can be utilized to probe the formation of intermediate species, charge separation upon illumination of sunlight and electron transfer to the interfacial reactions. A number of examples using soft x-ray spectroscopies to study these solar energy and catalytic materials are discussed to demonstrate how these powerful characterization tools could be helpful to further understand the energy conversion and energy storage systems.

Key words: in-situ/operando, soft x-ray spectroscopy, electronic structure, solar energy conversion, photoelectrochemical, interface

Corresponding author: Jinghua Guo (jguo@lbl.gov)

Sunlight provides very significant contribution to our electrical and chemical resources, if efficient and inexpensive systems utilizing are readily available through use of earth abundant materials that could be devised for the energy conversion processes. Solar energy, for example, can be converted to electricity and chemical fuels for energy use and storage [1-4]. Such a direct conversion of solar energy to electricity and fuels is important because it does not pollute (no acid rain or carbon dioxide emission, etc.). Moreover, there is much more solar energy available than needed, and it will be renewed as long as the sun shines. Another example is the development of catalysts that are capable of using sunlight to split water directly to generate hydrogen gas for fuel cell application. Unfortunately, the catalysts discovered so far that work under harsh chemical conditions with high efficiency are made from platinum, a rare and expensive metal.

An important example of the use of nanoporous materials was found many decades ago in the generation of H_2 and O_2 from direct photo-oxidation of water [5-6]. The demonstration experiments were performed on TiO_2, a large bandgap semiconductor which adsorbs only UV light. And energy conversion efficiency was on the order of 10^{-5}, which was too low for practical technology applications. The fabrication of artificial photosynthetic systems for the conversion of H_2O and CO_2 to fuels (for example, H_2 and CH_3OH) has become a field of much current research interest and has stimulated new fundamental investigations of the interaction of light, electron flow, and chemical reactions. Artificial photosynthetic processes start with the electron-hole pair formation that occurs at the interface between a semiconductor and a solution upon absorption of light and that leads to oxidation or reduction of solution species. Absorption depends on the band gap and band edge positions as well as the overall band structure of semiconductors, which are therefore of crucial importance in photoelectrochemical and photocatalytic applications (Figure 1).

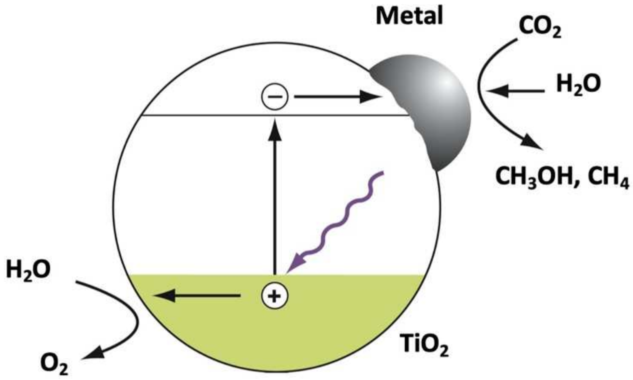

Figure 1. A diagram of electron-hole separation in semiconductor upon light adsorption (middle), the hole transport to participate the water oxidation reaction (left), and electron travels to catalytic site for reduction of carbon dioxide (right).

To succeed in splitting water using only solar radiation, the valence band of the semiconductor has to be located at a lower energy level than the chemical potential of oxygen evolution (H_2O/O_2), and the conduction band has to be located at a higher energy level than the chemical potential of hydrogen evolution (H_2/H^+). If the valence and conduction band energies do not fulfill this requirement, an external bias has to be applied to induce the photocatalytic process, which in turn substantially reduces the overall efficiency. [7]

There are, three fundamental requirements for any semiconducting catalytic system that converts and stores solar energy, expressible as three basic scientific challenges:

1) Efficient absorption of sunlight covering large fraction of the solar spectrum by semiconductors and molecules with bandgaps.

2) Electrons and holes created by absorption are sufficiently spatially separated to prevent recombination as well as suffer minimal loss of energy due to the scattering.

3) Photoexcited charges sufficiently energetic and mobile to drive a desired chemical transformation.

While utilizing solar energy will require new materials developed through the control of atomic, chemical, and electronic structure, achieving such control of properties requires an intimate collaboration between materials synthesis and characterization of the electronic properties of complex materials.

One of the crucial parameters for the use of semiconductors in solar cells is the bandgap ($E_{g,}$). In a semiconductor solar cell, electrons and holes — created when the solar photon energies exceed the bandgap — are pulled apart by the electric field between the p- and n-doped regions (see in Figure 2). [8] Voltage builds up until the conduction and valence bands flatten. The efficiency for the energy conversion and the cost are limiting factors. One requirement for achieving high efficiency is to avoid losing carriers during transport. Single-crystal semiconductors are better but expensive, while in-expensive polycrystalline thin-film materials lose carriers at grain boundaries.

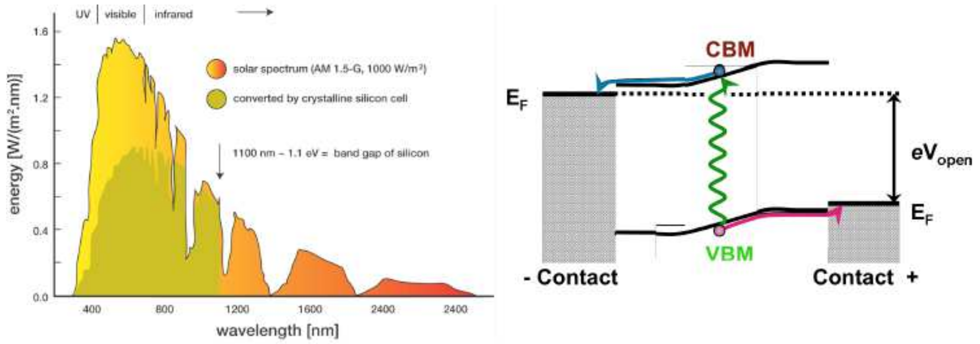

Figure 2. Solar light spectrum (left) and electron-hole pair in semiconductor (right [adopted from reference 8]). Generic energy level diagram of a solar cell, consisting of a light absorber sandwiched between an electron donor and an electron acceptor.

A second major factor limiting the conversion efficiency in single-bandgap cells to 31% is that the excess photon energy beyond the semiconductor bandgap is lost as heat through electron–phonon scattering and subsequent phonon emission while the carriers relax to their respective band edges (bottom of conduction band for electrons and top of valence for holes). The main approach for this loss in efficiency has been to use a stack of cascaded multiple p–n junctions with bandgaps better matched to the solar spectrum; in this way higher-energy photons are absorbed in the higher-bandgap semiconductors and lower-energy photons in the lower-bandgap semiconductors, thus reducing the overall heat loss due to carrier relaxation via phonon emission.

There are areas of fundamental research that the proposed facility will be in a unique position to address:

- Photovoltaics for Converting Sunlight to Electricity: To become competitive, rapid advances in fundamental understanding of thin film solar cell, dye-sensitized solar cell and polymer solar cells are essential. In addition, we need to explore other suitable photovoltaic materials that could provide reasonable efficiency by using only earth abundant materials that are easily manufacturable using industrial scalable processes.

- Artificial Photosynthesis for Converting Sunlight to Fuel: Nature has devised a remarkably diverse set of pathways to convert solar photons into chemical fuels. Learning from nature, we hope to create an artificial photosynthetic device, made from earth-abundant materials. We need to devise controlled experiments that allow better understanding for rate limiting steps of electrochemical processes such as functionality of fuel cell.

Soft x-ray spectroscopy probes the local unoccupied electronic structure; soft x-ray emission spectroscopy (XES) probes the local occupied electronic structure; and resonant inelastic soft x-ray scattering (RIXS) probes the low-energy excitations, such as charge transfer and proton-energy transfer. Synchrotron radiation-based soft x-ray spectroscopy has become a powerful tool to determine the band gap properties of semiconductors [9-10]. X ray absorption and emission both originate from an electronic transition between a localized core state and a valence state. Soft x-ray absorption probes the local unoccupied electronic structure (conduction band); soft x-ray emission probes the occupied electronic structure (valence band); and the addition of resonant inelastic soft x-ray scattering (Raman spectroscopy with soft x-rays) can tell the energy levels that reflect the chemical and physical properties of semiconductors, and probes the low-energy excitations, such as charge transfer and proton energy transfer [11-12]. Recently, quantum size effects on the exciton and band gap energies were observed in semiconductor nanocrystals [13-15]. If the observed valence band (VB) or conduction band (CB) shifts are due to quantum confinement, one would expect the size of the band shifts to increase as the particle size of the nanocrystals is decreased.

Soft x-rays are ideal for studying electron transitions between a localized core state and a valence/conduction state (see Figure 3), thus soft x-ray spectroscopy has unique features that make it a powerful tool to extract information about electronic properties [16-22]. Figure 3a illustrates the x-ray process in which a core electron is excited to the conduction band, followed by a valence electron decay to fill the core vacancy. Figure 3b shows an example of XAS and XES spectra revealing the metallic character of highly ordered 4pyrolytic graphite (HOPG) and the large bandgap or insulating character of diamond. In C K-edge absorption, the carbon 1s electron is excited to empty 2p electronic states in the carbon allotrope conduction band, and the dipole selection rule provides a tool to study locally the C 2p character of these unoccupied valence band. The atomic nature of the core hole implies elemental and site selectivity.

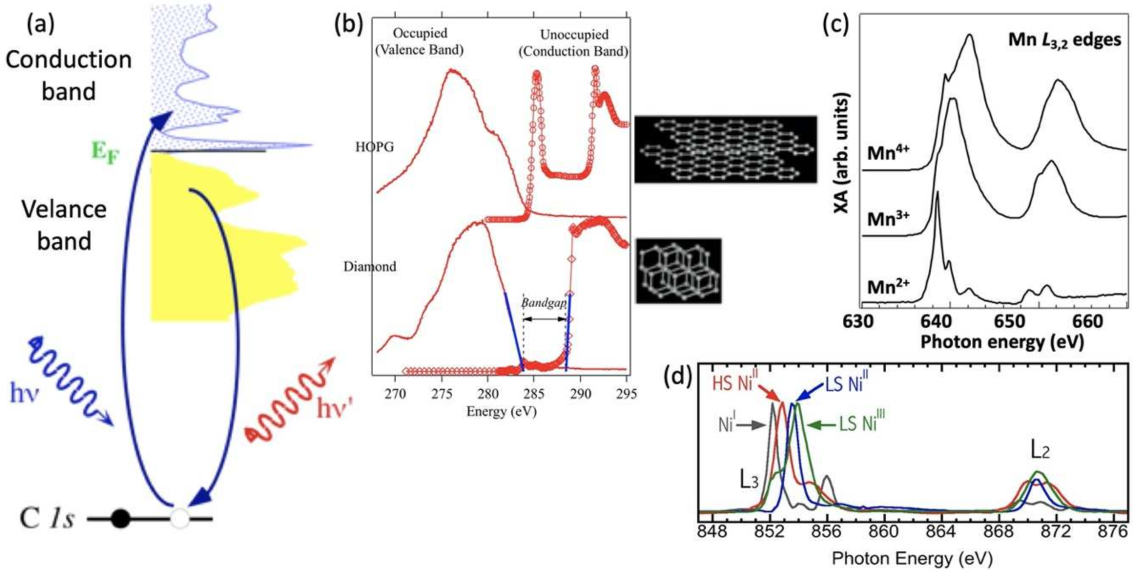

Figure 3. (a) A diagram of the carbon 1s electron is excited to empty 2p electronic states after adsorbing an x-ray photon and valence electron fill up the core hole and emit an x-ray photon, (b) C K-edge XAS and XES spectra of HOPG and diamond with both π and σ bonds in HOPG and only σ bond in diamond, (c) Mn L-edge XAS of different Mn oxidation states, (d) Ni L-edge XAS of different Ni oxidation states and also comparison of high-spin and low-spin states.

The Mn L-edge XAS spectra of different Mn compounds show different spectral profile in corresponding to the different oxidation states. The L_3 peak positions (and centroids) for these Ni complexes are 851.2 (851.3), 852.7 (853.1), 853.4 (853.4), and 853.9 (853.6) eV, respectively. [23] The L_3 resonances shift about 0.8 eV per oxidation state increase. Importantly, there is additional spectral information beyond the chemical shifts. The $Ni^{I}CO$ complex has a single L_3 peak, which is consistent with a d^9 configuration because there is only one 3d hole available in Ni^{I}. The peak at 856 eV is tentatively assigned to the mixed Ni−CO orbital. It is not surprising for some small ligand features following the L_3 main peak, especially for covalent ligands. The intense CO feature at 856 eV is due to the nature of the strong CO back-bonding and mixing with the 3d metal orbitals. This mixed orbital has Ni character and thus is observable with Ni XAS. At L_2, the main peak and the Ni−CO peak are closer to each other than those at L_3.

The LS Ni^{II} shows an absorption feature similar to $Ni^{I}CO$ (main peak), except the absorption peaks (centroids) are higher in energy positions. Although the LS Ni^{II} has a d^8 configuration, it has only one unfilled orbital level, resulting in a single L_3 peak. On the other hand, HS Ni^{II}, as exemplified by NiO, has two partially filled Ni 3d orbitals, leading to more complicated spectral features.

It is demonstrated that cobalt oxide nanoclusters are good candidates for water oxidation catalysts under mild pH and temperature conditions. O_2 yield is 1600 times higher for SBA-15/Co_3O_4 (35 nm) compared that of bare Co_3O_4 micron sized particles per weight [24]. Figure 4 shows a resonant inelastic soft x-ray scattering (RIXS) study of SBA15 (nanostructured Co_3O_4 in mesoporous silica) for water splitting to produce oxygen. A charge transfer (CT) excitation is identified, and the CT shows a variation in intensity when nanoporous silica is presented.

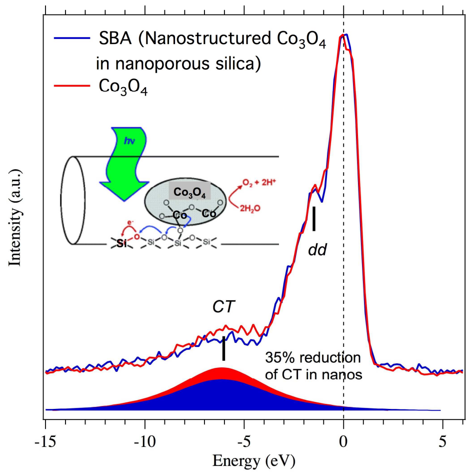

Figure 4. RIXS spectra of Co_3O_4 microcrystalline powder and nanostructured Co_3O_4 in nanoporous silica (SBA15).

The Co_3O_4 clusters formed inside the mesoporous silica (SBA-15) are ~35 and ~70 nm long for 4% and 8% weight loading, respectively. The spheroid shape clusters consist of parallel bundles of nanorods whose structure is imposed by the silica channels. The rods are linked by short bridges, formed by cobalt oxide growth in the micropores interconnecting the mesoscale channels.

Advances in the synthesis of particles of nanometer dimensions, narrow size distribution, and controlled shape have generated interest because of the potential to create novel materials with tailored physical and chemical properties [25,26]. New properties arise from quantum confinement effects and from the increasing fraction of surface atoms with unique bonding and geometrical configurations. Cobalt nanocrystals display a wealth of size-dependent structural, magnetic, electronic, and catalytic properties.

Soft x-rays are ideal for studying electron transitions between a localized core state and a valence/conduction state, thus soft x-ray spectroscopy has unique features that make it a powerful tool to extract information about electronic properties. Photon-in/photon-out soft x-ray spectroscopy can be used to study different chemical species of interest in depth under the real-world conditions, such as the presence of electric and/or magnetic fields and/or under gas catalytic reaction or liquid and electrochemical reaction conditions.

The electronic structure of cobalt nanocrystals suspended in liquid as a function of size has been investigated using in situ x-ray absorption and emission spectroscopy. A sharp absorption peak associated with the ligand molecules is found that increases in intensity upon reducing the nanocrystal size. X-ray Raman features due to d-d and to charge-transfer excitations of ligand molecules are identified. The study reveals the local symmetry of the surface of Co nanocrystals, which originates from a dynamic interaction between cobalt nanocrystals and surfactant + solvent molecules [27].

Figure 5 shows x-ray absorption spectra, Raman features of Co L_3-edge RIXS for cobalt nanocrystals of different diameters, and an illustration of the electron transfer from cobalt nanocrystals to the ligand molecules. The most notable feature in the spectra of the cobalt nanocrystals is the new absorption peak at 6 eV above the main absorption edge that is absent in the cobalt metal, CoO, Co_3O_4, and $CoCl_2$. This satellite peak is assigned as molecule–ligand charge transitions (MLCT) between cobalt and the oleic acid or 1,2-dichlorobezene.

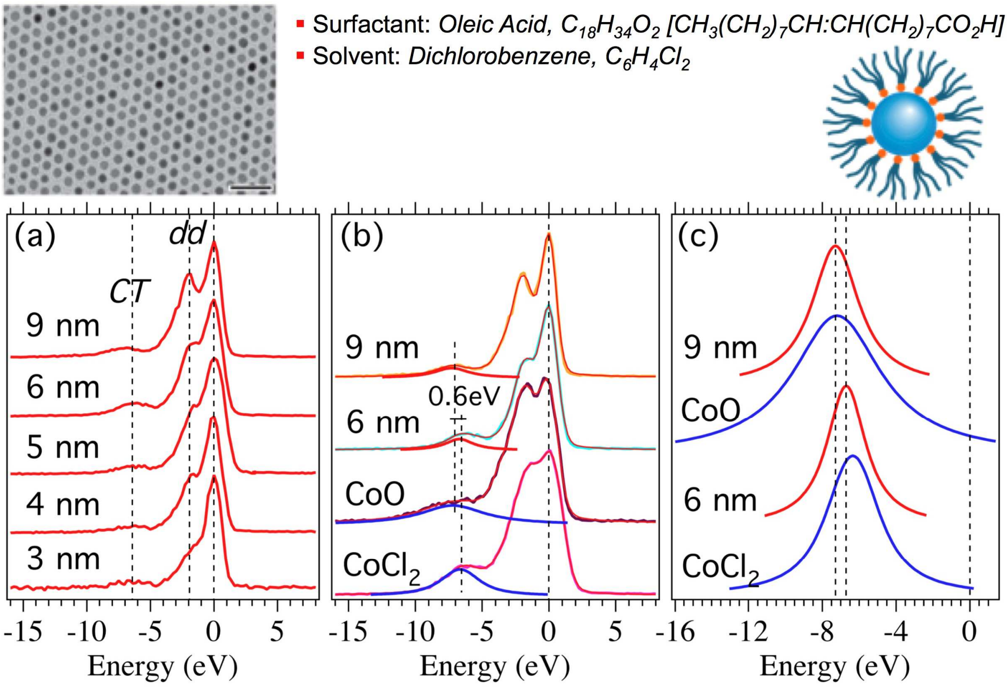

Figure 5. RIXS spectra of cobalt nanocrystal suspensions (a) peak fittings of RIXS spectra of cobalt nanocrystal and reference cobalt compounds (b) charge transfer peak of cobalt nanocrystal and cobalt reference compounds (c). [partially adopted from reference 27]

In cobalt metal, the ground state is $4s^2 3d^7$, while for CoO, one uses the ground state configuration $[3d^7 + 3d^8L^{-1}]$ (L^{-1} denotes a hole in the ligand level). Although this choice explained the CoO spectrum quite well, the $[3d^7 + 3d^8L^{-1}]$ configuration never yielded a significant satellite contribution, as seen in cobalt nanocrystals. The only known octahedral systems with large satellites are cyanide complexes, where large satellites are caused by π back-bonding, i.e., $[3d^7 + 3d^6L]$. The main structure is a $[2p^5 3d^8 + 2p^5 3d^7 L]$ bonding combination and the satellite is the antibonding part. It is worth noticing that the MLCT acts mainly on the t_{2g} electrons.

Figure 6 presents the principle design and the key features of the in-situ cells developed at Lawrence Berkeley National Laboratory. The static liquid cell, Figure 4(left) uses a thin membrane window to attain compatibility with UHV conditions of the experimental chamber [28,29, 30]. The x-ray beam enters the liquid cell through a 100 nm thick silicon nitride (Si_3N_4) window and the emitted x-rays exit through the same window. The membrane window opening is typically to be 1 mm × 1 mm in order to hold the liquid inside the cell in a vacuum environment which is required to perform soft x-ray experiments. Further-more, the electrochemical static liquid cell can be realized with embedded three electrodes for in-situ/operando soft x-ray spectroscopy experiments.

This design allows us to perform in-situ/operando electrochemistry x-ray spectroscopy measurements. The central part of the flow liquid cell (Figure 6 right) is similar to the static cell, while liquid flow allows a sample refresh to eliminate the sample damage problem It also allows changing the liquid conditions such as concentration, pH, temperature while performing soft x-ray spectroscopic measurements.

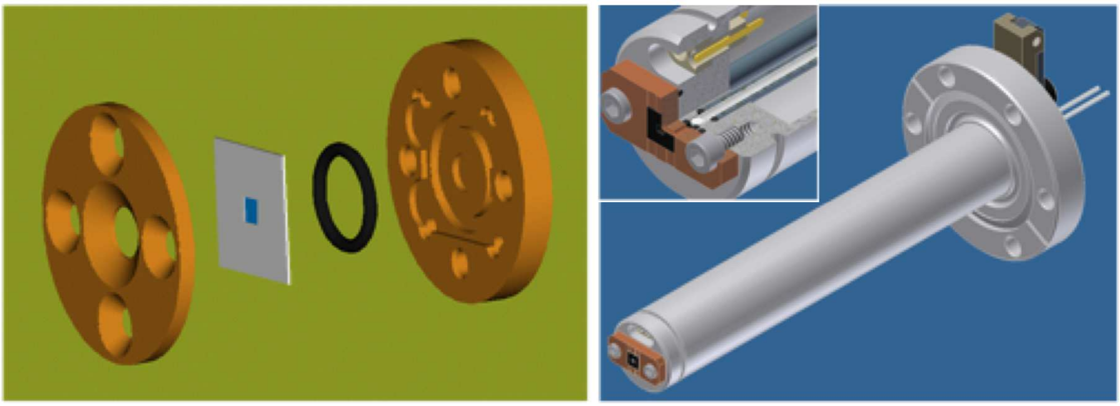

Figure 6. Static liquid cell (left) and flow liquid cell (right).

The understanding and control of electrochemical processes is particularly important in many cases ranging from batteries through potassium channels of cell membranes. The development of in-situ techniques gives rise to state-of-the-art studies on a number of different fields, such as catalysis, liquid and solution studies, etc. One major field, barely covered so far is the spectroscopic investigation of electrochemical systems in real time. As these cutting-edge experiments become available on BL7.3.1 and 8.0.1 at the ALS, we performed in-situ X-ray spectroscopic experiments (XAS, XES, RIXS) to probe the structural and chemical changes in deposited metal electrodes during cyclic voltammetric experiments.

Figure 7 shows the study of the structure and formation dynamics of the two different copper oxides (CuO, cupric oxide and Cu_2O, cuprous oxide) as a function of the electrode potential [31]. Cu L-edge XAS of Cu thin film on Si_3N_4 membrane before contacting any solution is shown in Figure 7 (right). The main component can be assigned to the L_3-edge (932.7 eV) of metallic Cu, consistent with the metallic Cu reference sample (Figure 7, XAS spectrum at the bottom). Except the main peak, there is one additional peak at the lower photon energy side (930 eV), which can be ascribed to Cu^{2+} species. The example show how in-situ/operando soft x-ray spectroscopy can become a valuable tool in renewable energy sciences, such as solar fuel generation. Challenges remain in the synthesis and characterization of photoelectrocatalysts. The role, played by the structure and dynamics of electron distributions in photoelectrochemical systems, is a fundamental but key property that in-situ/operando soft x-ray spectroscopy will be able to investigate.

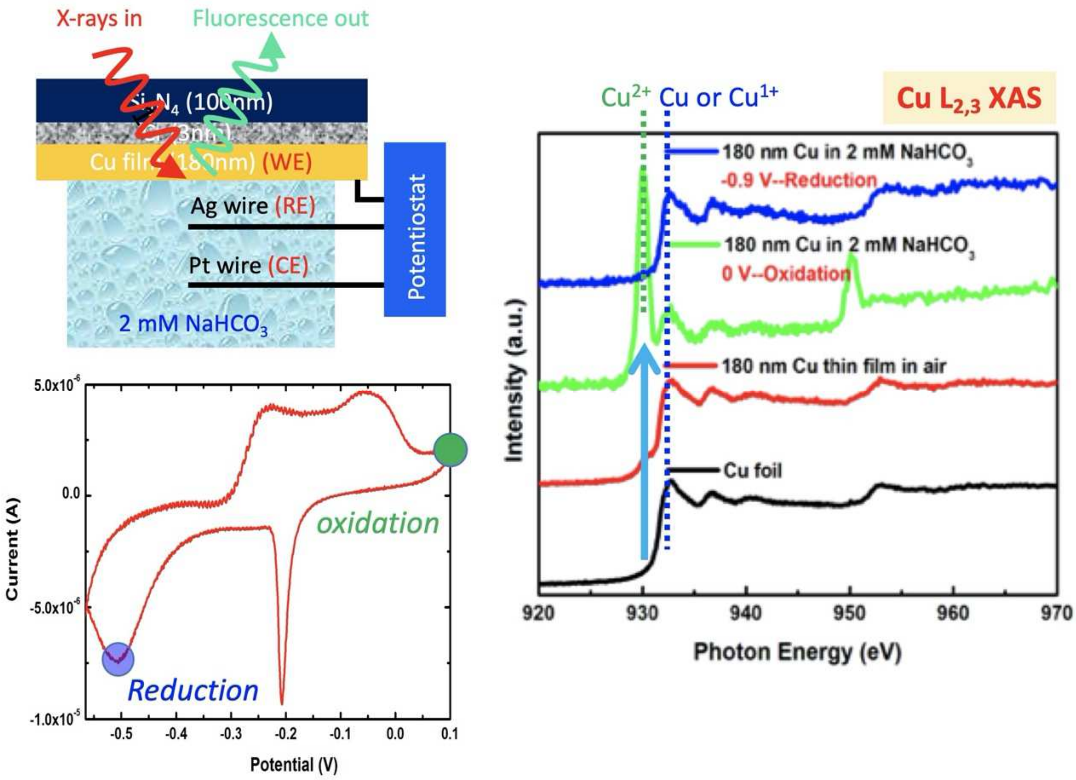

Figure 7. Left upper: illustration of electrochemical cell; Left bottom: Cu redox curve in 0.002 M Na_2CO_3 water solution; Right: XAS spectra of Cu electrode under oxidation/reduction condition. Reference metallic Cu foil together with the Cu thin film (~300 nm) evaporated on the Si_3N_4 membrane (oxidized during transfer in air). Spectra (3) and (4) were recorded after in-situ oxidation at nominally 0.2 V and after reduction at nominally −0.9 V in 2 mM $NaHCO_3$ solution, respectively.

In summary, soft x-ray spectroscopy can provide valuable information of chemical bonding and electronic structure of energy materials. In-situ/operando cells enable the soft x-ray spectroscopies as the powerful tools to probe the electronic structure of solid/liquid interfaces under chemical and electrochemical reactions. Insights derived from the cutting-edge characterization are valuable to develop new solar energy conversion and storage systems. One important scientific hurdle – understanding the intermediate states that occur during catalytic processes – can be addressed with in-situ/operando synchrotron techniques.

Acknowledgements

The authors gratefully acknowledge research support from the Hydrogen Materials Advanced Research Consortium (HyMARC), established as part of the Energy Materials Network by the U.S. Department of Energy, Office of Energy Efficiency and Renewable Energy, Fuel Cell Technologies Office. The x-ray spectroscopy experiments discussed were performed on BL7.3.1 (XAS endstation) and BL8.0.1.4 (wetRIXS endstation) at the Advanced Light Source, which is supported by the Office of Science of the U.S. Department of Energy under Contract No. DE-AC02-05CH11231.

References

[1] G. W. Crabtree and N. S. Lewis, Solar Energy Conversion, Physics Today 60 (2007) 37-42.

[2] J. R. Bolton, S. J. Strickler, and J. S. Connolly, Limiting and realizable efficiencies of solar photolysis of water, Nature 316 (1985) 495.

[3] A. J. Bard, Photoelectrochemistry, Science 207 (1980) 139-144.

[4] J. R. Bolton, Solar Fuels, Science 202 (1978) 705-711.

[5] A. Fujishima and K. Honda, Electrochemical Photolysis of Water at a Semiconductor Electrode, Nature 238 (1972) 37-38.

[6] T. Inoue, A. Fujishima, S. Konishi, and K. Honda, Photoelectrocatalytic reduction of carbon dioxide in aqueous suspensions of semiconductor powders, Nature 277 (1979) 637-638.

[7] Z. Zhou, J. Ye, K. Sayama, and H. Arakawa, Direct splitting of water under visible light irradiation with an oxide semiconductor photocatalyst, Nature 414 (2001) 625-627.

[8] F.J. Himpsel, P.L. Cook, G. de la Torre, J.M. Garcia-Lastra, R. Gonzalez-Moreno, J.-H. Guo, R.J. Hamers, C.X. Kronawitter, P.S. Johnson, J.E. Ortega, D. Pickup, M.-E. Ragoussi, C. Rogero, A. Rubio, R.E. Ruther, L. Vayssieres, W. Yang, I. Zegkinoglou, Design of solar cell materials via soft X-ray spectroscopy, J. Electr. Spectr. Relat. Phenom. 190 (2013) 2-11.

[9] J.-H. Guo, Synchrotron radiation, soft-X-ray spectroscopy and nanomaterials, Int. J. Nanotechnology 1-2 (2004) 193-225.

[10] J.-H. Guo, X-ray Absorption and Emission Spectroscopy in Nanoscience and Lifesciences, pp. 259-291, in Nanosystem characterization Tools in the Life Sciences, edited by Challa Kumar, Wiley-VCH Verlag GmbH & Co. KgaA, Weinheim (2006).

[11] P. Kuiper, J.-H. Guo, C. Såthe, L.-C. Duda, J. Nordgren, J. J. M. Pothuizen, F. M. F. de Groot, and G. A. Sawatzky, X-ray Resonant Raman Spectra of Cu dd Excitations in Sr_2CuOCl_2, Physical Review Letters 80 (1998) 5204.

[12] B. Freelon, A. Augustsson, J.-H. Guo, P. G. Medaglia, A. Tebano, and G. Balestrino, Electron Correlation and Charge Transfer in $[(Ba_{0.9}Nd_{0.1})CuO_{2+d}]_2/[CaCuO_2]_2$ Superconducting Superlattices, Physical Review Letters, 96 (2006) 017003.

[13] T. van Buuren, L. N. Dinh, L. L. Chase, W. J. Siekhaus, and L. J. Terminello, Changes in the Electronic Properties of Si Nanocrystals as a Function of Particle Size, Phys. Rev. Lett. 80 (1998) 3803.

[14] K. S. Hamad, R. Roth, J. Rockenberger, T. van Buuren, and A. P. Alivisatos, Structural Disorder in Colloidal InAs and CdSe Nanocrystals Observed by X-Ray Absorption Near-Edge Spectroscopy, Phys. Rev. Lett. 83 (1999) 3474.

[15] J.-Y. Raty, G. Galli, C. Bostedt, T. van Buuren, and L. J. Terminello, Quantum Confinement and Fullerenelike Surface Reconstructions in Nanodiamonds, Phys. Rev. Lett. 90 (2003) 37401.

[16] A. Kotani and S. Shin, Resonant inelastic x-ray scattering spectra for electrons in solids, Review of Modern Physics 73 (2001) 203.

[17] Y. Ma, N. Wassdahl, P. Skytt, J.-H. Guo, J. Nordgren, P. D. Johnson, J-E. Rubensson, T. Bske,W. Eberhardt, and S. D. Kevan, Soft X-ray Resonant Inelastic Scattering at the C K Edge of Diamond, Phys. Rev. Lett. 69 (1992) 2598.

[18] P. Glans, K. Gunnelin, P. Skytt, J.-H. Guo, N. Wassdahl, J. Nordgren, H. Ågren, F. Kh. Gel'mukhanov, and T. Warwick, Resonant X-ray Emission Spectroscopy of Molecular Oxygen, Phys. Rev. Lett. 76 (1996) 2448.

[19] P. Skytt, P. Glans, J.-H. Guo, K. Gunnelin, C. Såthe, J. Nordgren, F. Kh. Gel'mukhanov, A. Cesar, and H. Ågren, Quenching of Symmetry Breaking in Resonant Inelastic X-ray Scattering by DetunedExcitation, Phys. Rev. Lett. 77 (1996) 5035.

[20] P. Kuiper, J.-H. Guo, C. Såthe, L.-C. Duda, J. Nordgren, J. J. M. Pothuizen, F. M. F. de Groot, and G. A. Sawatzky, X-ray Resonant Raman Spectra of Cu dd Excitations in Sr_2CuOCl_2, Phys. Rev. Lett. 80 (1998) 5204.

[21] J.A. Carlisle, E.L. Shirley, E.A. Hudson, L.J. Terminello, T.A. Calcott, J.J. Jia, D.L. Ederer, R.C.C. Perera, and F.J. Himpsel, Probing the Graphite Band Structure with Resonant Soft-X-Ray Fluorescence, Phys. Rev. Lett. 74 (1995) 1234.

[22] J.-H. Guo and J. Nordgren, Resonant C Kα X-ray emission of some carbon allotropes and organic compounds, J. Electr. Spectr. Rel. Phenom. 110-111 (2000) 105-134.

[23] H. Wang, S. M. Butorin, A. T. Young, and J.-H. Guo, Nickel Oxidation States and Spin States of Bioinorganic Complexes from Nickel L-edge X-ray Absorption and Resonant Inelastic X-ray Scattering, J. Phys. Chem. C 117 (2013) 24767−24772.

[24] F. Jiao and H. Frei, Nanostructured Cobalt Oxide Clusters in Mesoporous Silica as Efficient Oxygen-Evolving Catalysts, Angew. Chem. 121 (2009) 1873.

[25] G. Somorjai and Borodko, Research in Nanosciences – Great Opportunity for Catalysis Science, Catal. Lett. 76 (2001) 1.

[26] Z. Konya, V. F. Puntes, I. Kiricsi, J. Zhu, A. P. Alivisatos, G. A. Somorjai, Novel Two-Step Synthesis of Controlled Size and Shape Platinum Nanoparticles Encapsulated in Mesoporous Silica, Catal. Lett. 81 (2002) 137-140.

[27] H. Liu, J.-H. Guo, Y. Yin, A. Augustsson, C. Dong, J. Nordgren, C. Chang, P. Alivisatos, G. Thornton, D. F. Ogletree, F. G. Requejo, F. de Groot, and M. Salmeron, Electronic Structure of Cobalt Nanocrystals Suspended in Liquid, Nano Lett. 7 (2007) 1919-1922.

[28] J.-H. Guo, T. Tong, L. Svec, J. Go, C. L. Dong, and J.-W. Chiou, Soft-x-ray Spectroscopy Experiment of Liquids, J. Vac. Sci. Technol. A 25 (2007) 1231-1233.

[29] Y.-S. Liu, S. Jeong, J. L. White, X. Feng, E. S. Cho, V. Stavila, M. D. Allendorf, J. J. Urban, and J.-H. Guo, In-situ/operando X-ray characterization of metal hydrides, ChemPhysChem 20 (2019) 1261-1271.

[30] C. L. Dong and L. Vayssieres, In Situ/Operando X-ray spectroscopies for advanced investigation of energy materials, Chemistry-A European Journal 24 (2018) 18356-18373.

[31] P. Jiang, J.-L. Chen, F. Borondics, P.-A. Glans, M. W. West, C.-L. Chang, M. Salmeron, J.-H. Guo, In situ soft X-ray absorption spectroscopy investigation of electrochemical corrosion of copper in aqueous $NaHCO_3$ solution, Electrochemistry Communications 12 (2010) 820-822.

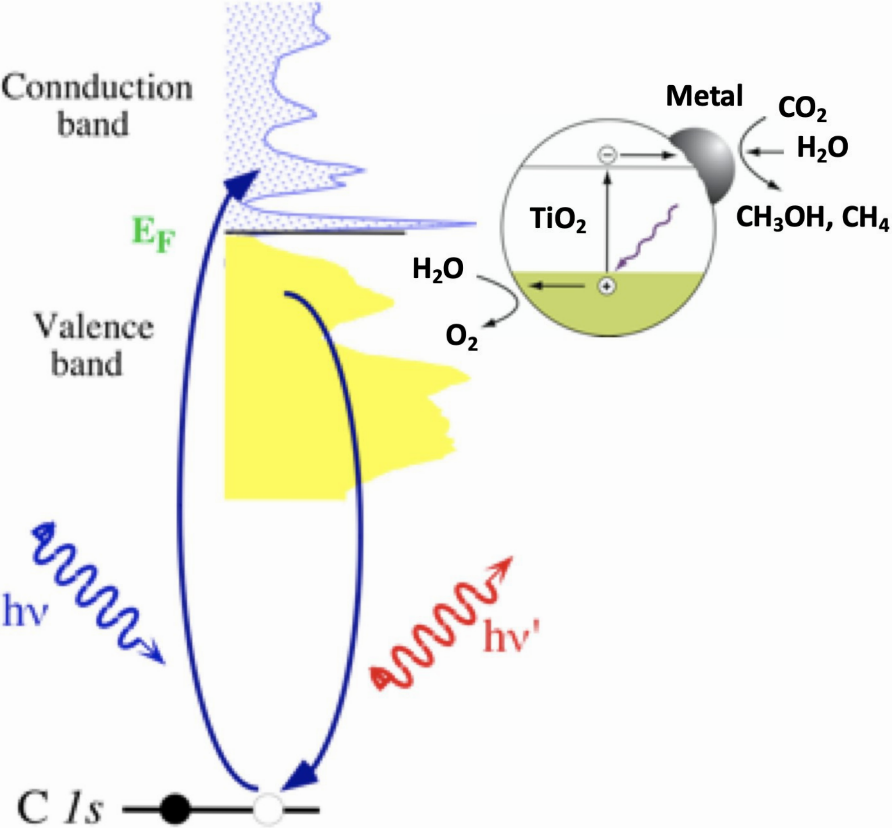
Connduction band
E$_F$
Valence band
hv
hv'
C 1s
Metal
CO$_2$
H$_2$O
TiO$_2$
CH$_3$OH, CH$_4$
H$_2$O
O$_2$